

Tracking the Solid-Electrolyte-Interphase (SEI) formation on amorphous Si and Sn anodes for Li-ion batteries

J.R. Kim^{*†}, M. Doucet^{*}, J.F. Browning[†], G.M. Veith^{**}

^{*}Neutron Data Analysis & Visualization Division, Oak Ridge National Laboratory, Oak Ridge, TN

[†]Chemical & Engineering Materials Division, Oak Ridge National Laboratory, Oak Ridge, TN

^{**}Materials Science & Technology Division, Oak Ridge National Laboratory, Oak Ridge, TN

ABSTRACT

Neutron reflectometry provides a detailed method in which to investigate the solid-electrolyte interphase (SEI) throughout its initial formation and under dynamic cycling conditions in lithium-ion batteries. Amorphous silicon (a-Si) and tin are investigated to demonstrate both the thickness and scattering length density of the SEI layer considering a fluoroethylene carbonate (FEC) electrolyte additive. Distinct differences and similarities between the two systems have been identified; both a-Si and Sn observe a reversible contraction/growth of the SEI layer throughout charge/discharge cycles originating from the buildup and dissolution of organic components at the electrolyte surface. a-Si observes a clear tendency to form an initial $\text{Li}_2\text{O}/\text{Li}_2\text{CO}_3$ layer based on a chemical reaction that occurs between the native oxide and the electrolyte prior to electrochemical cycling. Whereas the native tin oxide appears to remain intact, forming an SEI of different composition as a result.

Keywords: lithium, batteries, solid-electrolyte-interphase, neutron reflectometry, electrochemistry

1 INTRODUCTION

Lithium-ion batteries have been widely developed over decades with special emphasis on electrode composition and bulk electrochemical processes. However, the scope of study investigating the interfacial reaction(s) occurring at the electrode surfaces is comparatively small. The solid-electrolyte interphase (SEI) is a protective layer which forms on the electrode surface, preventing unwanted reduction of the electrolyte within the normal operating voltages of the electrochemical cell. The SEI is a critical battery component, itself preventing continual capacity fade and potential safety concerns surrounding the formation of gaseous products among a range of other concerted processes that take place under normal operating conditions.

Silicon and tin anodes are attractive next-generation energy storage materials, and have been under investigation for a number of years [1–4]. Despite their high theoretical capacities, differences in their interfacial properties (w.r.t. graphite) lead to a number of unexpected changes in SEI chemistry, identifying the need to study interfacial reactions at the electrode surface(s) on a case-by-case basis. The SEI is composed of inorganic and organic species that are formed

on the electrode surface *via* electroreduction of the electrolyte and chemical reaction(s) occurring with the native oxide(s) on the electrode surface [5]. Controlling the SEI has been completely limited to systematically investigating a range of electrolyte compositions and electrolyte additives designed to preferentially decompose onto the electrode surface, forming a conformal and passivating layer on the electrode surface [6–8]. This method of optimization proves to be a very slow and arduous endeavor considering the simultaneous need to find an electrolyte composition that is also stable against the positive electrode and aluminum current collector, and which is also stable within the desired electrochemical window prompting the need for a greater understanding of SEI chemistry and methodologies in which to control its behavior.

The studies described herein investigate both the static and dynamic nature of the SEI throughout its initial formation and throughout reversible cycling. Neutron Reflectometry (NR) provides a powerful method for the investigation of both soft matter and solid-liquid interfaces, drawing an important connection between the native oxide(s) formed on electrode surfaces and their interaction with the liquid electrolyte. Here, both amorphous silicon (a-Si) and tin (Sn) are investigated for lithium-ion battery applications utilizing a fluoroethylene carbonate electrolyte additive. A pathway for future investigations examining the role of oxynitride/nitride surface treatments is also identified, providing a potential method in which the morphology and composition of the SEI can be tailored to meet desired applications.

2 MATERIALS AND METHODS

2.1 Thin Film Fabrication

Thin film samples were fabricated *via* DC/RF magnetron sputtering using an in-house sputtering system onto either battery grade copper foil or Si substrates. 2" diameter (5 mm thick) single crystal Si substrates were used without removal of their native oxide for NR measurements.

Film thicknesses were monitored using a quartz crystal microbalance and kept under vacuum throughout successive depositions to prevent the formation of native oxides between the current collector and Si/Sn layer. Cu (99.99%, Kurt J. Lesker), Si (99.999%, Kurt J. Lesker), Cr (99.95%, Kurt J. Lesker), and Sn (99.99% Kurt J. Lesker) targets were

used as purchased. Silicon anode samples comprise a Cu and a-Si layer of thicknesses *ca.* 70 Å and 450 Å respectively. Tin anode samples were fabricated using Cr and Sn layer thicknesses of *ca.* 100 Å and 400 Å respectively. Layer thicknesses were chosen based on theoretical reflectometry data and to maximize the contrast of the SEI layer. Actual samples contain slight variations from these numbers.

2.2 Characterization

Neutron reflectometry (NR) measurements were conducted on the Liquids Reflectometer (BL-4B) at the Spallation Neutron Source (SNS) at Oak Ridge National Laboratory (ORNL). The Liquids Reflectometer is a time-of-flight reflectometer utilizing an effective single bandwidth of 3.5 Å at a pulse frequency of 60 Hz. A momentum transfer range of 0.008 \AA^{-1} to 0.22 \AA^{-1} is achieved from utilizing neutron wavelengths from 2.5 Å – 17 Å at four incident angles of $\theta = 0.60^\circ, 0.69^\circ, 1.37^\circ,$ and 2.71° . Incident beam slit heights are varied to allow a constant beam footprint (39 mm x 21 mm). Data reduction and absolute normalization is performed using Mantid [9] and the resulting reflectivity profiles are analyzed and modeled using Motofit [10].

X-ray photoelectron spectroscopy (XPS) was performed on a PHI 3056 spectrometer with an Al anode source operating at 15 kV and an applied power of 350 W. XPS measurements were collected using 23.5 and 93.5 eV high and low resolutions respectively. XPS measurements were conducted on thin film samples deposited onto battery grade Cu foil before and after electrochemical cycling.

2.3 Electrochemical Measurements

Electrochemical measurements were performed on a-Si and Sn anodes in CR2032 type coin cells (Cu foil samples) and using a custom electrochemical reflectivity cell similar to that shown in Figure 1. Electrical connections to the reflectometry samples was made by applying a silver epoxy to the substrate prior to deposition to which an external wire is soldered onto.

Electrolytes using both ^1H and ^2H were used to provide additional contrast against the SEI. Protiated and deuterated ethylene carbonate (EC), dimethyl carbonate (DMC), and fluoroethylene carbonate (FEC - protiated) were obtained from Sigma Aldrich and dried with 5 Å molecular sieves in an Argon filled glovebox. 1M LiPF_6 EC/DMC (3:7 wt% respectively) and 1M LiPF_6 EC/DMC/FEC (27.5:67.5:5 wt% respectively) electrolyte compositions were used. Electrochemical experiments were run on a Biologic VSP potentiostat. All reported voltages are relative to Li/Li^+ .

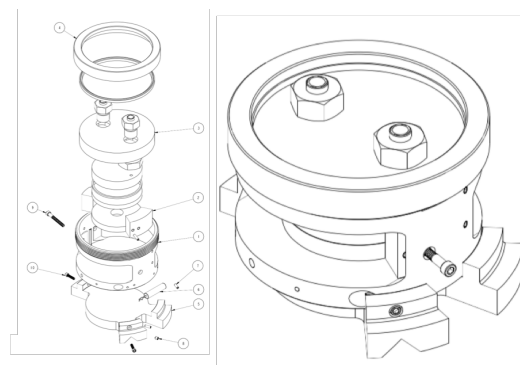


Figure 1: Schematic of electrochemical reflectometry cell.

3 RESULTS AND DISCUSSION

3.1 Amorphous Silicon Anodes

Figure 2 provides the neutron reflectometry data taken on an a-Si anode with air as an incident medium, assembled in the electrochemical cell at open circuit voltage, and at a nominal half-cell potential of 0.21 V (vs Li/Li^+). A combination of protiated (not shown) and deuterated solvents were utilized to provide significantly different scattering length density (SLD) values (*ca.* $1.6 \times 10^{-6} \text{ \AA}^{-2}$ and $5.6 \times 10^{-6} \text{ \AA}^{-2}$ respectively) to clearly identify the relative contributions of inorganic/organic components within the SEI.

Additional measurements made at 1.5 V, 0.9 V, and 0.6 V (not shown) demonstrate a consistent trend throughout the a-Si samples. Namely, the native oxide on the a-Si electrode is entirely absent once beginning measurements at OCV, accompanied by a successive etching of the a-Si surface within the OCV – 0.6 V range. Here, etching of the a-Si surface is sensible, as minor moisture contamination is expected considering both the [relatively low] purity of the deuterated solvents and initial characterization in air prior to assembly in the electrochemical cell. Cells utilizing protiated solvents see comparatively lower amounts of etching, supporting the suspected moisture contamination.

Throughout these initial measurements, both NR and XPS indicate that the formation of a dense $\text{Li}_2\text{O/Li}_2\text{CO}_3$ passivating layer is formed ranging between 20 – 40 Å in thickness (Fig 2 a-c). The contrast between the protiated and deuterated electrolytes further clarifies the predominantly inorganic nature of this SEI precursor, as only minor contributions from the ^1H and ^2H containing compounds can be seen throughout the SEI. Throughout the discharge reaction the diverging nature of the SLD between the protiated and deuterated electrochemical cells demonstrate that the SEI becomes considerably more oligomeric/polymeric as components of the electrolyte begin to be reduced at the electrode surface.

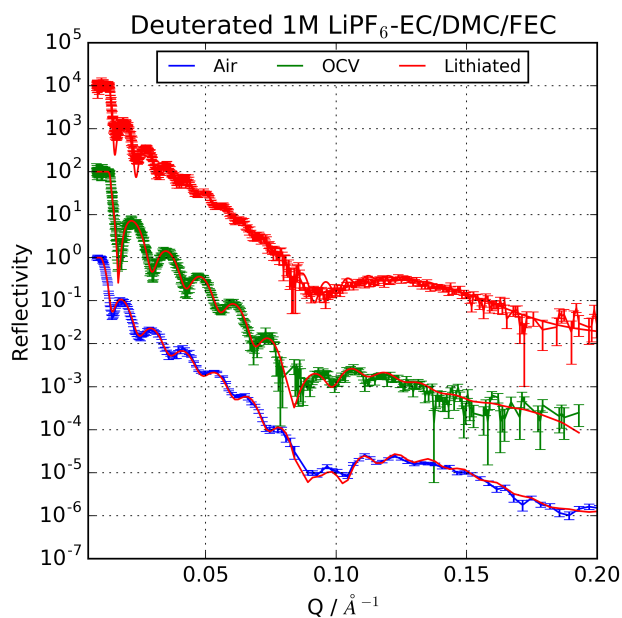


Figure 2: Neutron reflectometry data and respective model fits on amorphous silicon anode samples and schematic of thin film sample throughout the air, OCV, and lithiated measurements. Once assembled into the electrochemical cell, consumption of the native oxide and portions of the underlying a-Si layer is observed (a) – (c) forming an initial SEI composed primarily of inorganic components. Upon insertion of Li into the a-Si anode, the layer thickness increases, and the SEI shows a change in composition.

Complementary *ex situ* XPS measurements show a distribution of Li_2CO_3 , Li_2O and LiF products within the SEI precursor layer along with the thickening of the SEI layer throughout the discharge reaction, which are in good agreement with NR experiments.

3.2 Tin anodes

Initial reflectometry data on the dynamic behavior of the SEI on Sn anodes is given in Figure 2. Here, NR measurements are provided for those taken in air, in the electrochemical cell after a 0.05 V discharge (lithiated), and after charging to 1.0 V (delithiated). In the case of Sn, the role of the native oxide is considerably more complex, itself being electrochemically active. [12] While initial investigations into the interfacial reactions occurring between the native oxide/electrolyte are ongoing, a discrete SEI layer forming on top of the native oxide can be seen; appearing to

be drastically different from the conversion-type reaction as seen in the case of a-Si, potentially indicating the formation of an Li_xSiO_y interfacial layer.

As lithium is inserted into the Sn/SnO_x electrode, the layer thickness increases to *ca.* 1400 Å and then contracts back to *ca.* 500 Å after charging indicating that only partial delithiation has taken place. In the fully lithiated state, the SEI is relatively thick (compared to a-Si) at *ca.* 160 Å; eventually decreasing to *ca.* 60 Å after delithiating to 1.0 V; in agreement with the ‘breathing’ characteristic seen for a-Si.[13]

Although further work utilizing protiated electrolytes to determine relative contributions of inorganic/organic SEI compositions is needed, it is reasonable to expect that there are similar compositional changes occurring between the fully charged and discharged states. That is to say the SEI composition oscillates between being predominantly inorganic/organic in the fully delithiated/lithiated states respectively.

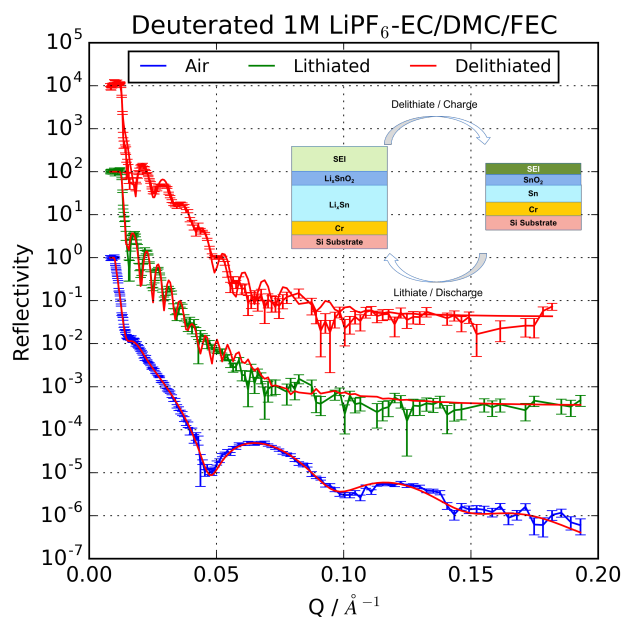


Figure 2: Neutron reflectometry data and respective model fits on tin anode samples and schematic of the changing thickness/SLD of the SEI between the lithiated and delithiated states (inset figure).

3.3 Tin nitride thin films

As the native tin oxide has demonstrated a potentially different fundamental route towards the initial SEI formation step, additional chemical doping of the near surface region is of particular interest.

Initial measurements on tin nitride films have been performed in air in order to investigate the quality of as-made films and demonstrate their ability to prevent the formation of a native oxide. Figure 3 provides the reflectometry data and SLD profile of the multilayer film. The SnOH layer (< 20 Å) depicted in Figure 3 is formed as a result of

adsorbed moisture on the nitride surface. The stoichiometry of the SnN_x layer ($\text{Sn}_{2.6}\text{N}_{3.2}$) are based on estimates from XPS and NR measurements.

Previous *in situ* electrochemical measurements suggest a correlation between the surface composition of the electrode and the resulting SEI that forms on its surface. The latter stage(s) of SEI formation are believed to be largely influenced by ways in which this SEI precursor layer interacts with the electrolyte, and is the topic of future investigations. Controlling the SEI composition *via* chemical treatments of the electrode surface may prove to hold increased safety implications and potentially allow for drastically simpler electrolytes due to the potentially higher passivating nature of engineered SEI precursor layers.

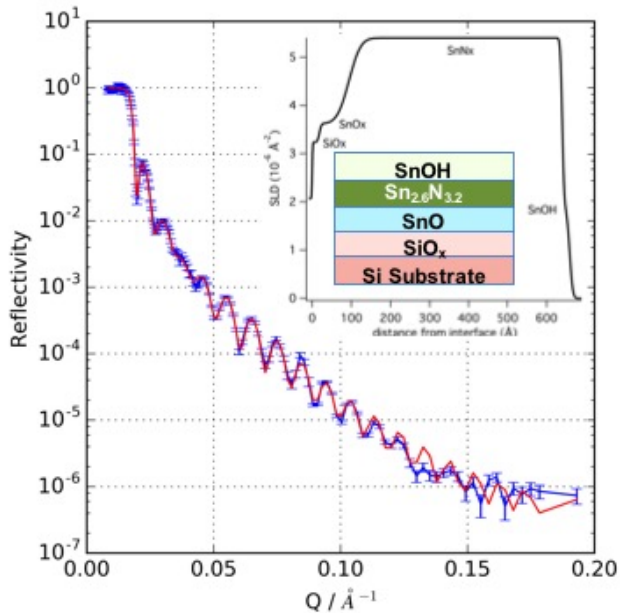


Figure 3: Neutron reflectometry and model fit of tin nitride thin film. Inset scattering length density profile and schematic of thin film structure.

4 CONCLUSION

The behavior of the SEI demonstrates considerable sensitivity to both the specific electrode chemistry employed and the coinciding electrolyte(s) used. Throughout the Li^+ alloying/dealloying process, both a-Si and Sn exhibit a constantly changing nature of the SEI in terms of both its characteristic thickness and overall composition as summarized in Table 1. Overall, the SEI consists of a thick layer with a large fraction of organic components (resulting from the solvent/salt) upon reaching full lithiation, and a thin, predominately inorganic layer after delithiation has taken place.

Initial characterization on tin nitride thin films has demonstrated the ability to fabricate high quality thin film samples. Additional studies investigating the use of Sn, SnO_x , and SnN_x interfaces to control the SEI chemistry are currently underway. This technique goes beyond traditional

encapsulation type layers, providing an alternative approach towards controlling SEI chemistry.

	SEI precursor	Lithiated SEI	Delithiated SEI
a-Si	20 – 40 Å conversion of native oxide	Thick SEI: growing amount of organics	Thin SEI: More inorganic
Sn	Under investigation	Thick SEI: large amount of organics	Thin SEI: predominantly inorganic

Table 1: Summary of the SEI characteristics for a-Si and Sn cycled against Li/Li^+ .

REFERENCES

- [1] Han; Li; Hu. *Nano Lett.* **2013**, *13*, 3093–3100.
- [2] Leblanc; Hovington; Kim; Guerfi; Bélanger; Zaghbi. *J. Power Sources* **2015**, *299*, 529–536.
- [3] Wachtler; Besenhard; Winter. *J. Power Sources* **2001**, *94* (2), 189–193.
- [4] Chevrier; Dahn. *J. Electrochem. Soc.* **2009**, *156* (6), A454–A458.
- [5] He et al. *ACS Nano* **2014**, *8* (11), 11816–11823.
- [6] Wagner; Brox; Kasnatscheew; Gallus; Amereller; Cekic-Laskovic; Winter. *Electrochem. commun.* **2014**, *40*, 80–83.
- [7] Eom; Jung; Lee; Lair; Joshi; Lee; Lin; Fuller. *Nano Energy* **2015**, *12*, 314–321.
- [8] Schmitz et al. *Prog. Solid State Chem.* **2014**, *42* (4), 65–84.
- [9] Arnold et al. *Nucl. Instruments Methods Phys. Res. Sect. A Accel. Spectrometers, Detect. Assoc. Equip.* **2014**, *764*, 156–166.
- [10] Nelson. *J. Appl. Crystallogr.* **2006**, *39*, 273–276.
- [11] Asay; Kim. *J. Phys. Chem. B* **2005**, *109* (35), 16760–16763.
- [12] Lu; Ma; Alvarado; Kidera; Dimov; Meng; Okada. *J. Power Sources* **2015**, *284*, 287–295.
- [13] Veith; Doucet; Baldwin; Sacci; Fears; Wang; Browning. *J. Phys. Chem. C* **2015**, *119* (35), 20339–20349.